Available online at www.sciencedirect.com
SCIENCE DIRECT®
Journal of the European Ceramic Society 25 (2005) 1507–1514
www.elsevier.com/locate/jeurceramsoc

Preparation and characterization of novel bioactive dicalcium silicate ceramics

Zhongru Gou, Jiang Chang*, Wanyin Zhai

Biomaterials and Tissue Engineering Research Center, Shanghai Institute of Ceramics, Chinese Academy of Sciences, 1295 Dingxi Road, Shanghai 200050, PR China

Received 8 March 2004; received in revised form 13 May 2004; accepted 23 May 2004
Available online 12 August 2004

Abstract

The *beta*- and *gamma*-dicalcium silicate (β- and γ-Ca_2SiO_4) ceramics were prepared by sintering β-Ca_2SiO_4 greens at 1100, 1300, and 1450 °C, respectively, after compacting with cold isostatic pressure. The phase transition from β- to γ-phase of polymorphic ceramics occurred at 1100–1300 °C. Bending strength and Vickers hardness of β-Ca_2SiO_4 ceramic sintered at 1100 °C were only 25.6 ± 3.8 MPa and 0.41 ± 0.05 GPa. In contrast, the mechanical properties of the γ-Ca_2SiO_4 were improved remarkably when the ceramics were sintered at 1450 °C, corresponding to bending strength, 97.1 ± 6.7 MPa; Vickers hardness, 4.34 ± 0.35 GPa, respectively. The ceramics were soaked in the simulated body fluid (SBF) for various periods were characterized by SEM, XRD, FTIR, and EDS analysis, and the results indicated that the carbonated hydroxyapatite (CHA) was formed on the surface of the ceramics within 3 days. In addition, cell attachment assay showed that the ceramics supported the mesenchymal stem cells adhesion and spreading, and the cells established close contacts with the ceramics after 1 day of culture. These findings indicate that the γ-Ca_2SiO_4 ceramic possesses good bioactivity, biocompatibility and mechanical properties, and might be a promising bone implant material.

Keywords: Bioactivity; Biocompatibility; Mechanical properties; Silicates; Ca_2SiO_4

1. Introduction

Bioactive ceramics in medicine have become one of the major fields in biomaterials over the last three decades. One remarkable success of bioactive ceramics as implant materials is the clinical use of sintered hydroxyapatite (HA) due to its bioactivity and osteoconductivity.[1–4] However, the low fracture toughness of HA ceramic limit the scope of clinical applications.[4–6] In recent years, more attentions have been focused on developing novel bioactive ceramics with improved properties. More recently, extensive interests have been shown in developing new bioactive inorganic materials containing CaO–SiO_2 component for biomedical applications, i.e., bioactive glasses,[7–9] $CaSiO_3$ ceramics[10] and A/W glass-ceramics.[11,12] These CaO–SiO_2 containing ceramics with different mechanical properties have shown excellent bioactivity when immersed in simulated body fluid (SBF) or implanted into the bone defect.[13,14]

Traditionally, dicalcium silicate (Ca_2SiO_4) is an important constituent in Portland cement, refractories and heat-resistant coatings.[15–18] Recent studies have shown that Ca_2SiO_4 has the potential to be used as biomaterials. Liu et al.[19] prepared Ca_2SiO_4 coatings on the Ti alloys and a bonelike carbonated hydroxyapatite (CHA) layer formed on the surface of the coatings when soaked in SBF for 2 days. In addition, we have also demonstrated that β- and γ-Ca_2SiO_4 powders possessed good bioactivity in SBF environment.[20] However, to our knowledge, the preparation of characterization of the Ca_2SiO_4 ceramics have not yet been reported. In this context, the objectives of this work were to fabricate novel Ca_2SiO_4 ceramics and to investigate the sintering behavior, mechanical properties, bioactivity, and biocompatibility of the ceramics.

* Corresponding author. Tel.: +86 21 52412804; fax: +86 21 52413903.
E-mail address: jchang@mail.sic.ac.cn (J. Chang).

0955-2219/$ – see front matter © 2004 Elsevier Ltd. All rights reserved.
doi:10.1016/j.jeurceramsoc.2004.05.029

2. Materials and methods

2.1. Preparation of Ca_2SiO_4 ceramics

The β-Ca_2SiO_4 powders were prepared according to a modified sol–gel process,[20] and were characterized by X-ray diffraction (XRD, Rigaku Co., Japan). Free CaO content in the powders was determined by the glycol–ethanol method.[21] The Ca_2SiO_4 ceramics were fabricated by sintering the β-Ca_2SiO_4 green compacts at different temperatures. The green samples were prepared by mechanically mixing the β-Ca_2SiO_4 powders with 6 wt.% polyvinyl alcohol (PVA124; aqueous solution) as binder. The binder-to-powder ratio was optimized as 5/95 (w/w) to minimize the negative effect of the binder on the densification and mechanical properties of the sintered ceramics. All green compacts were formed by uniaxially pressing the mixture either in a rectangular mould (45 mm × 8 mm) or a cylindrical mould (Ø 10 mm), followed by cold isostatic pressing (CIP) at 200 MPa to improve their densification. The sintering was performed at 1100, 1300, and 1450 °C for 2 h, respectively, in a high- temperature furnace at a heating rate of 2 °C min^{-1} and then furnace cooled naturally.

2.2. Characterization of the as-prepared ceramics

Parts of the disk-shaped samples were crushed for XRD analysis. Linear shrinkage of the sintered rectangular samples after sintering was determined using the following equation:

$$\text{Shrinkage} = \frac{l_g - l_p}{l_g} 100\%$$

where l_g is the length of green samples and l_p the length of sintered products. Apparent density measurement was performed on each sample by Archimedes' method in order to evaluate the degree of densification of the sintered ceramics. The mass of samples was determined using an electric balance and the relative density (RD) is calculated by the following equation:

$$\text{RD} = \frac{\rho_a}{\rho_t} 100\%$$

where ρ_t and ρ_a are theoretical density and apparent density of the samples, respectively.

2.3. Evaluation of mechanical properties

Vickers hardness (H_v) of the Ca_2SiO_4 ceramics was evaluated by a Vickers indentation technique (Hardness tester, AKASHI, Japan) using a loading of 49 N on the samples. Six indentations were made on polished surface perpendicular to the height direction. The measurement of the compressive strength (σ_c) was performed on the sintered ceramic disks (Ø 10 mm) with a universal-testing machine (Instron-1195, USA); the three-point bending strength (σ_f) and Young's modulus (E) were measured by the same machine at a crosshead speed of 0.5 mm min^{-1} and a span of 30.0 mm according to the ASTM C1259-95 standard. The fracture toughness (K_{IC}) was estimated with the help of three-point bending measurement according to the procedure reported previously.[22] Measurements were performed at room temperature using the rectangular-shaped samples (40.0 mm × 6.0 mm × 3.0 mm) with a notch width of less than 150 μm. The ratio between notch depth and sample thickness was 0.5. Eight replicates of each material were determined and the results were expressed as mean ± standard deviation.

2.4. Soaking in SBF

The ceramic disks sintered at 1100 and 1450 °C, respectively, were placed in polystyrene bottles containing SBF with ion concentrations nearly equal to human blood plasma as shown in the previous publication.[23] The bottles with SBF and samples were incubated at 37.0 °C in a shaking water bath for predetermined intervals with a surface area-to-volume ratio of 0.1 cm^{-1} [24] without refreshing the soaking medium. After different soaking periods the disks were removed from SBF, rinsed with deionized water, and dried at room temperature. Surface structure and morphology of the soaked specimens were characterized by XRD, Fourier transformed-infrared spectroscopy (FTIR; Nicolet Co., USA) and scanning electron microscopy (SEM; JSM-6700F, JEOL, Japan). Compositional changes on cross-section of the Ca_2SiO_4 disk at 1450 °C were identified by SEM-associated energy-dispersive spectrum (EDS).

2.5. Cell adhesion assay

Primary bone marrow-derived mesenchymal stem cells (MSCs) from newborn calf femur were isolated and cultured using the method described by Ringe et al.[25] For this study only the MSCs at the second–third passage were employed. The Ca_2SiO_4 ceramic disks were sterilized under ultraviolet light and followed by washing with sterile phosphate-buffered saline (PBS; pH 7.4). Then, the cells were seeded onto the disks at a density of 3.0×10^4 cells/well in a 48-well culture plate in 1 ml Dulbecco's modified eagle's medium (DMEM). The culture was maintained at 37 °C, 5% CO_2 in a humid atmosphere. After incubation for 6 h and 1 day, respectively, part of disks were removed from the culture wells, rinsed with PBS twice and fixed with 10% formalin solution for 30 min. After fixation, the disks were dehydrated in a grade ethanol series ((v/v); 70% for 10 min, 95% for 10 min and 100% for 20 min). The samples were treated using the alcohol–HMDS (hexamethyldisilizane; Shanghai Chemical Reagent Co.) solution,[26] and finally air dried in a desiccator overnight. The specimens were then sputter-coated with gold and viewed by SEM. The other disks were rinsed with PBS twice, placed in 10% formalin solution for 30 min and strained with hematoxylin and eosin (H&E) for observation using light microscopy.

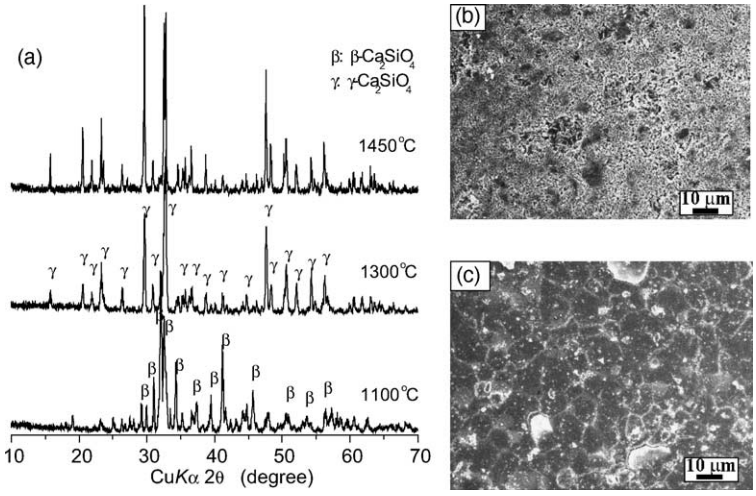

Fig. 1. XRD patterns (a) and SEM micrographs of β-Ca_2SiO_4 ceramics (b), and γ-Ca_2SiO_4 ceramics (c).

Table 1
Physical structure of the Ca_2SiO_4 ceramics sintered at different temperatures

Physical structure	Sintering temperature (°C)		
	1100	1300	1450
Linear shrinkage (%)	5.98 ± 0.11	16.94 ± 0.31	22.62 ± 0.20
Relative density (%)	88.84 ± 0.70	93.30 ± 0.52	96.17 ± 0.34

3. Results

3.1. Ceramic preparation and characterization

Fig. 1(a) shows the XRD patterns of the as-prepared Ca_2SiO_4 ceramics sintered at different temperatures. It is clear to see from the diffraction patterns that the ceramics remained β-phase when the green compacts were sintered at 1100 °C, while it transformed into γ-phase over 1300 °C, indicating that a phase transition occurred between 1100 and 1300 °C. Fig. 1(b and c) show the SEM micrographs of surfaces of the β- and γ-Ca_2SiO_4 ceramics sintered at 1100 and 1300 °C, respectively. It is obvious that the β-Ca_2SiO_4 ceramic had a rougher surface with irregular pores, as compared to that of the γ-Ca_2SiO_4 ceramic, which presented compact microcrystalline appearance with clear crystal boundaries.

In addition, shrinkage and densification were evaluated as a part of physical property measurement to understand the sintering behavior of these ceramics. From Table 1, it can be seen that the linear shrinkage and relative density of the ceramics sintered at 1100 °C were 5.98 and 88.84% respectively, while for the ceramics sintered at 1300–1450 °C they attained 16.94–22.62 and 93.30–96.17%, respectively. It is obvious that the increase of sintering temperatures drastically promoted pore filling and ceramic densification, which was also in agreement with the surface observation by SEM in Fig. 1.

3.2. Mechanical property evaluation

Table 2 lists the mechanical properties of the Ca_2SiO_4 ceramics sintered at different temperatures. Notably by increasing sintering temperature up to 1450 °C, very high bending strength and Vickers hardness were produced (∼97.1 MPa and ∼4.34 GPa), whereas equivalent samples sintered at 1100 °C yielded ceramic with 25.6 MPa bending strength and 0.41 GPa Viskers hardness. Moreover, the Young's modulus (E), fracture toughness (K_{IC}) and compressive strength (σ_c) of the Ca_2SiO_4 ceramics were improved remarkably after phase transition into γ-Ca_2SiO_4. An increase in sintering

Table 2
Mechanical properties of the dicalcium silicate, sintered HA and cortical bone

Material	Vickers hardness, H_v (GPa)	Young's modulus, E (GPa)	Fracture toughness, K_{IC} (MPa $m^{1/2}$)	Bending strength, σ_f (MPa)	Compressive strength, σ_c (MPa)
β-Ca_2SiO_4 ceramic[a]	0.41 ± 0.05	10.4 ± 2.2	1.12 ± 0.11	25.6 ± 3.8	148.5 ± 10.1
γ-Ca_2SiO_4 ceramic[b]	3.62 ± 0.28	34.0 ± 1.5	1.48 ± 0.09	78.9 ± 8.2	172.9 ± 12.0
γ-Ca_2SiO_4 ceramic[c]	4.34 ± 0.35	40.2 ± 3.2	1.80 ± 0.07	97.1 ± 6.7	200.6 ± 8.9
Sintered HA	6.0	80–120	1.0	115–200	500–1000
Cortical bone	–	7–30	2–12	50–150	113–193

[a] Sintered at 1100 °C.
[b] Sintered at 1300 °C.
[c] Sintered at 1450 °C.

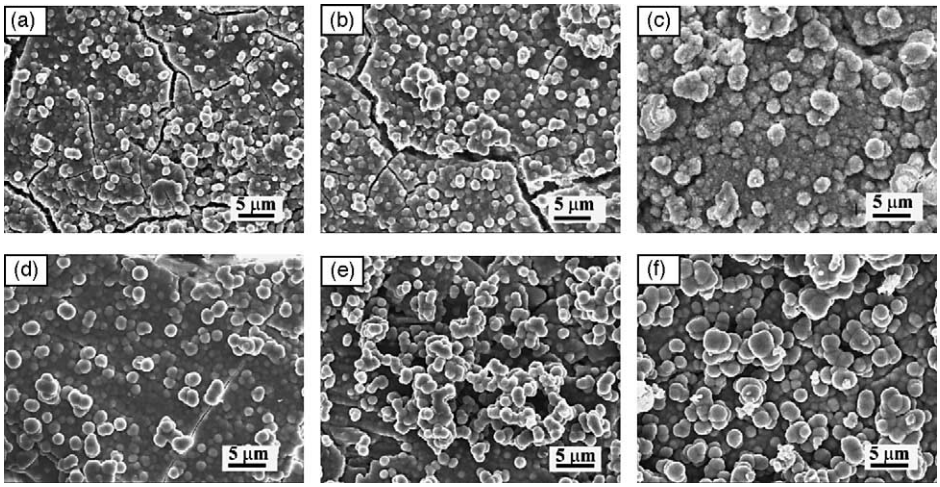

Fig. 2. The SEM micrographs of the β-Ca_2SiO_4 ceramics (a–c) and γ-Ca_2SiO_4 ceramics (d–f), soaked in SBF for 6 h (a and d), 1 day (b and e) and 3 days (c and f).

temperature up to 1450 °C resulted in an increase of E from 10.4 to 40.2 GPa, K_{IC} from 1.12 to 1.80 MPa $m^{1/2}$ and σ_c from 148.5 to 200.6 MPa, respectively.

3.3. Formation of CHA on the surface of Ca_2SiO_4 ceramics

The surface morphologies of the ceramics after soaking in SBF are shown in Fig. 2. After soaking for 6 h, some heterogeneous particles were deposited on the surface of β- and γ-Ca_2SiO_4 ceramics (Fig. 2(a and d)). With the increase of soaking time up to 3 days, a crystalline layer thought to be HA covered the whole disks (Fig. 2(c and f)). The XRD analysis (Fig. 3) showed that the characteristic peaks of HA were appeared accompanied with the deposition of some $CaCO_3$ after soaking for 3 days. Concurrently, the peaks of Ca_2SiO_4 deceased remarkably and Ca_2SiO_4 transformed into a calcium silicate hydrate (C-S-H; PDF # 29.0379) due to the hydration of Ca_2SiO_4 in the aqueous solution.

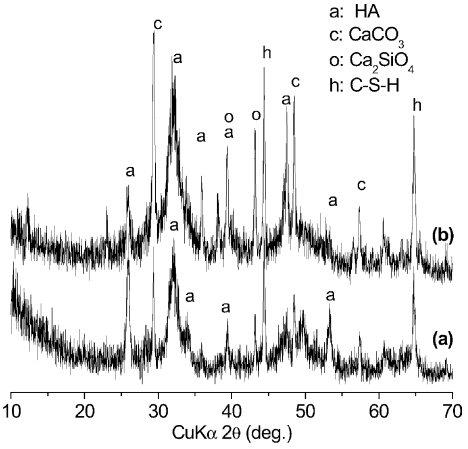

Fig. 3. XRD patterns of the β-Ca_2SiO_4 ceramics (a) and γ-Ca_2SiO_4 ceramics (b) after soaking in SBF for 3 days.

Fig. 4 shows FTIR spectra of the β- and γ-Ca_2SiO_4 ceramic disks before and after soaking in SBF. In the spectra before soaking (Fig. 4, 0 h), the absorption bands of silicate groups were evident. The intense band at 980 cm^{-1} was assigned to the Si–O–Si asymmetric stretch, the band at 910–880 cm^{-1} to the Si–O symmetric stretch, and the band at 510 cm^{-1} to the Si–O–Si vibrational mode of bending. After 6 h soaking, two bands appeared at 568 and 1035 cm^{-1} that could be assigned to the P–O vibrational mode of an amorphous phosphate. After 1 and 3 days, the FTIR spectra were analogous to that of the synthetic bonelike CHA, where the bands at 1035, 601, and 568 cm^{-1} could be assigned to the phosphate (PO_4^{3-}), and those at 1453, 1419, and 872 cm^{-1} to the carbonate (CO_3^{2-}).[27]

Fig. 5 illustrates SEM micrograph and EDS spectra of the polished cross-section of the γ-Ca_2SiO_4 ceramic soaked in SBF for 10 days. It is clear to see from the SEM micrograph and linear EDS spectra (Fig. 5(a)) that two layers with different compositions were observed on the surface of the ceramic. The top layer was 7–8 μm thick and rich in Ca and P as shown by EDS analysis. The Ca/P ratio was 1.72, which was close to the ratio of 1.67 for HA (Fig. 5(b)). A silica-rich layer with a thickness of 10 μm was identified by EDS analysis, in which the Ca/Si ratio of 0.19 (Fig. 5(c)). Fig. 5(d) showes γ-Ca_2SiO_4 ceramic matrix with a Ca/Si ratio of 1.99.

3.4. Adhesion of MSCs on the ceramics

Figs. 6 and 7 show the morphology of MSCs adhering and spreading on the β- and γ-Ca_2SiO_4 ceramic disks after culturing for 6 h and 1 day. From Fig. 6, it can be seen that the cells adhered onto the surface of the disks and the spreading morphology of the cells could be observed on the ceramics after 6 h in culture. In addition, it is obvious from the SEM micrographs (Fig. 7) that the cells mainly presented a close contact with the ceramic surface and thin cytoplasmic digitations could be seen after 6 h (Fig. 7(a and b)). However,

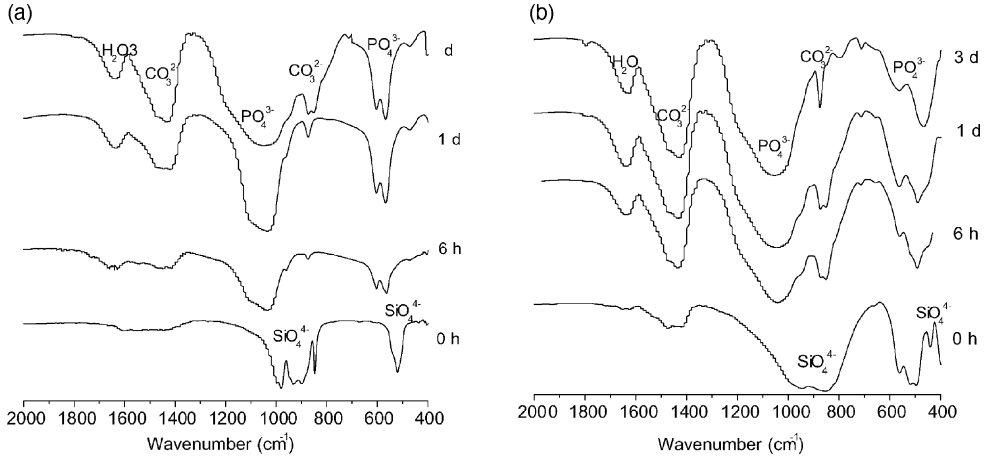

Fig. 4. FTIR spectra of the β-Ca_2SiO_4 ceramics (a) and γ-Ca_2SiO_4 ceramics (b) after soaking in SBF for various time periods.

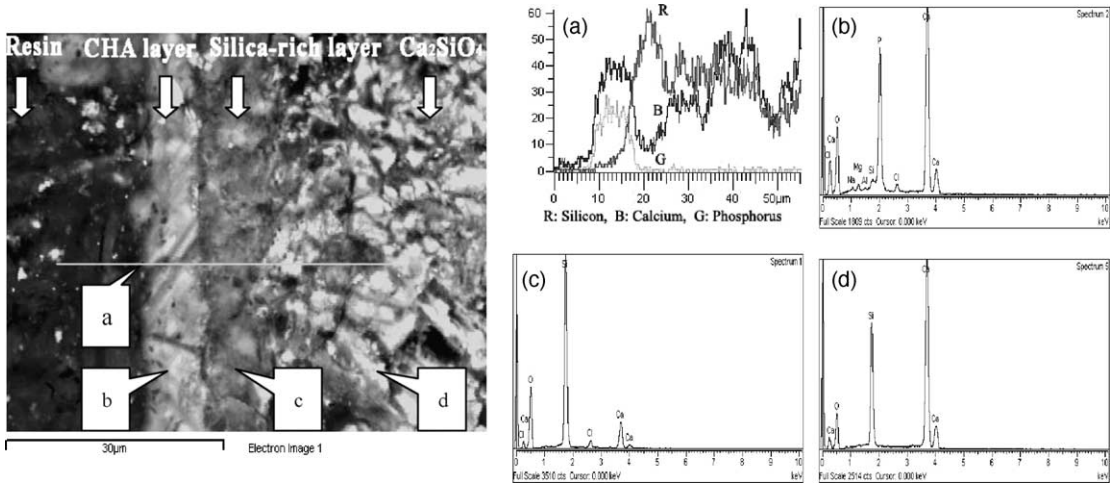

Fig. 5. SEM micrograph and EDS of a cross-section of the γ-Ca_2SiO_4 ceramic embedded in epoxy resin after soaking in SBF for 10 days. (a) EDS spectra along a line, (b) EDS spectra at a point in the CHA layer, (c) EDS spectra at a point in the silica-rich layer, and (d) EDS spectra at a point in the ceramic substrate.

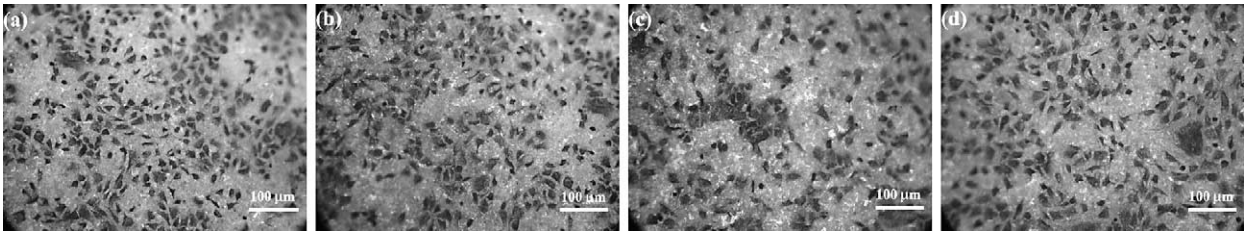

Fig. 6. Light micrographs of the MSCs cultured on β-Ca_2SiO_4 (a and c) and γ-Ca_2SiO_4 (b and d) disks for 6 h (a and b) and 1 day (c and d) after seeding.

cytoplasm webbing of the cells were evident and filopodia projected progressively on the γ-Ca_2SiO_4 at day 1 (Fig. 7(d)).

4. Discussion

In recent years, multiple interests in Ca_2SiO_4 have been extended to many fields of silicate science, coating materials and refractories. There are five normal polymorphs of Ca_2SiO_4, of which the most important are the stable γ-phase and metastable β-phase at ambient temperature.[28] Our results in this work showed that the β-Ca_2SiO_4 ceramics could be prepared by sintering the β-phase green compacts at 1100 °C and the γ-Ca_2SiO_4 could be obtained at a temperature above 1300 °C. Previous studies showed that Ca_2SiO_4 experienced considerable grain volume changes throughout

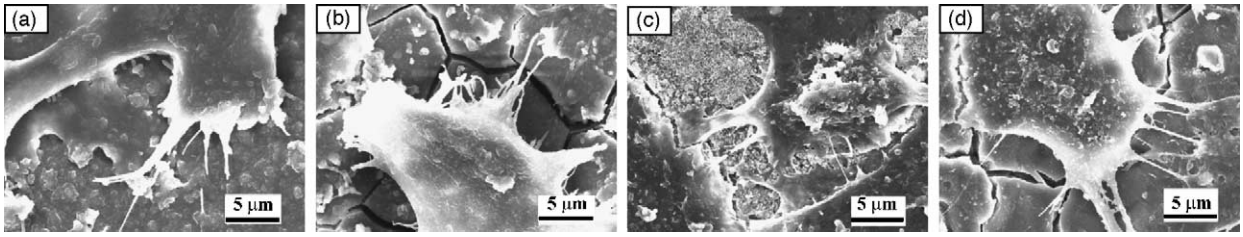

Fig. 7. Morphological aspects of MSCs spreading on β-Ca_2SiO_4 (a and c) and γ-Ca_2SiO_4 (b and d) disks for 6 h (a and b) and 1 day (c and d) by SEM.

the phase transition, especially, a shrinkage of ∼11.2% from α (at 1425 °C) to β (at room temperature) and a large volume increase of ∼12.3% during the β → γ transition (at room temperature).[29,30] In single-phase β-Ca_2SiO_4, the euhedral β grains were highly strained and grain growth gave rise to a development of microcracks along the grain boundaries, whereas such microcracks could be refrained and the grain size remained stable during the β → γ transition at a short sintering time.[30] Accordingly, the dense γ-Ca_2SiO_4 ceramic can be fabricated by sintering the β-polymorph green at 1450 °C.

A key requirement for the clinical success of the bioactive ceramics is emphasized to a match of the mechanical behavior of the implant with the tissue to be replaced, and in most cases, the goal is to increase strain to failure and decrease elastic modulus.[31–34] According to the loading sharing principle of the composite theory,[35] the bioactive ceramics with overhigh *E* modulus are liable to induce bone resorption owing to the stress shielding that surrounds them. Thus, it is expected to fabricate the bioactive ceramics with *E* modulus analogous to that of human bone. The mechanical properties of the Ca_2SiO_4 ceramics are shown in Table 2 together with the published data of the cortical bone and sintered HA used clinically.[32] As compared to the β-Ca_2SiO_4 ceramic, the γ-Ca_2SiO_4 ceramic revealed the improved mechanical properties. This can be attributed to the transformation toughening mechanism produced by the β → γ transition induced by the stress field at the microcracks.[36] The toughness characteristic of ceramics plays a significant role in the fracture mechanism. The higher the K_{IC} value is, the better is the mechanical behavior of an implant fabricated out of this material. The γ-Ca_2SiO_4 ceramics sintered at 1450 °C showed an improvement on the K_{IC} values (1.80 MPa $m^{1/2}$) as compared to the sintered HA (K_{IC} = ∼1.0 MPa $m^{1/2}$). Likewise, the *E* modulus of the γ-Ca_2SiO_4 was markedly lower than that of the sintered HA, but close to the cortical bone. Previous studies have shown that the mechanical strengths of the sintered ceramics were correlated with the densification.[37,38] In our study, the relative density obtained for γ-Ca_2SiO_4 ceramic was only 96.17%, which suggest that a further improvement of the mechanical properties might be possible by the novel super-fast consolidation technique, spark plasma sintering[39] which might lead to a further increase of the densification of the γ-Ca_2SiO_4 ceramic.

It is a common notion that bonelike CHA plays an essential role in the formation, growth and maintenance of the bone tissue-biomaterial interface, and this CHA layer can be reproduced in vitro in an acellular SBF.[23,40] The present study showed that the Ca_2SiO_4 ceramics induced the formation of a silica-rich layer and a CHA layer was developed on the surface of the silica-rich layer in SBF. Previous investigations have shown that a silica-rich layer could be identified when bioactive glasses were soaking in SBF, and Hench[41] have proposed that the hydrated silica-rich layer provided specific favorable sites for CHA formation. Therefore, our results suggest that the mechanism of CHA formation on the surface of Ca_2SiO_4 ceramics is similar to that for bioactive glasses and can be interpreted as follows. The ionic exchange between Ca^{2+} ions in Ca_2SiO_4 ceramic and H_3O^+ ions in SBF increased the degree of supersaturation of the surrounding fluid, and made a favorable hydrated silica gel layer on the ceramics, which can in turn attract the phosphate groups, creating amorphous calcium phosphates, and then the eventual coverage of the entire surface with crystalline bonelike CHA layer by incorporating CO_3^{2-} and OH^- ions from SBF.

Some studies demonstrate that the bone marrow-derived MSCs show strong estrogenic potential and form new bone on the porous bioactive ceramics within 2 weeks after implantation.[42,43] In this work, we evaluated the biocompatibility of β- and γ-Ca_2SiO_4 ceramics by examining the MSCs adhesion. It was observed that after seeding cells on the ceramics, the cells underwent their morphological changes to stabilize the cell-biomaterial interface, and the cells spread and established close contacts with the β- and γ-Ca_2SiO_4 ceramics, adapting a flattened morphology and showing numerous filopodia anchoring the cells to the bioactive ceramics after 1 day. These results indicate that the β- and γ-Ca_2SiO_4 ceramics support the cell adhesion.

5. Conclusions

The novel β- and γ-Ca_2SiO_4 ceramics can be fabricated by sintering the β-Ca_2SiO_4 green compacts at different temperatures. The mechanical properties of the ceramics are dependent significantly on sintering temperature and phase transition, and the γ-Ca_2SiO_4 better mechanical property compared to the β-Ca_2SiO_4 phase. The Young's modulus, compressive and bending strength of the γ-Ca_2SiO_4 sintered at 1450 °C are close to that for the cortical bone. The in vitro studies show that β- and γ-Ca_2SiO_4 ceramics induced

formation of a CHA layer in SBF within 3 days and supported osteogenic cells adhesion and spreading. Because of its characteristics, the γ-Ca_2SiO_4 ceramic might be a promising candidate as implant materials.

Acknowledgment

This work was financially supported by Science and Technology Commission of Shanghai Municipality under grant no: 02JC14009.

References

1. Ohgushi, H., Goldberg, V. M. and Caplan, A. I., Hetrotopic osteogenesis in porous ceramics induced by marrow cells. *J. Orthop. Res.*, 1989, **7**, 568–578.
2. Stephenson, P. K., Freeman, M. A., Revell, P. A., Germain, J., Tuke, M. and Pirie, C. J., The effect of hydroxyapatite coating on ingrowth of bone into cavities of an implant. *J. Arthroplasty*, 1991, **6**, 51–58.
3. Guan, J. L. and Chen, H. C., Signal transduction in cell–matrix interactions. *Int. Rev. Cytol.*, 1996, **168**, 82–121.
4. Shores, E. C. and Holmes, R. E., Porous hydrozyapatite. In *An Introduction to Bioceramics*, ed. L. L. Hench and J. Wilson. World Scientific, Singapore, 1993, pp. 181–198.
5. LeGeros, R. Z. and LeGeros, J. P., Dense hydroxyapatite. In *An Introduction to Bioceramics*, ed. L. L. Hench and J. Wilson. World Scientific, Singapore, 1993, pp. 139–180.
6. Suchanek, W. and Yoshimura, M., Processing and properties of hydroxyapatite-based biomaterials for use as hard tissue replacement implants. *J. Mater. Res.*, 1998, **13**, 94–117.
7. Izquierdo-Barba, I., Salinas, A. J. and Vallet-Regí, M., In vitro calcium phosphate formation on sol–gel glasses of the CaO–SiO_2 system. *J. Biomed. Mater. Res.*, 1999, **47**, 243–250.
8. Izquierdo-Barba, I., Salinas, A. J. and Vallet-Regí, M., Effect of the continuous solution exchange on the in virto reactivity of a CaO–SiO_2 sol–gel glass. *J. Biomed. Mater. Res.*, 2000, **51**, 191–199.
9. Salinas, A. J., Vallet-Regí, M. and Izquierdo-Barba, I., Biomimetic apatite deposition on calcium silicate gel glasses. *J. Sol–gel Sci. Technol.*, 2001, **21**, 13–25.
10. Siriphannon, P., Kameshima, Y., Yasumori, A., Okada, K. and Hayashi, S., Influence of preparation conditions on the microstructure and bioactivity of α-$CaSiO_3$ ceramics: formation of hydroxyapatite in simulated body fluid. *J. Biomed. Mater. Res.*, 2000, **52**, 30–39.
11. Kokubo, T., Ito, S., Huang, Z. T., Hayashi, T., Sakka, S., Kitsugi, T. *et al.*, Ca, P-rich layer formed on high-strength bioactive glass-ceramic A-W. *J. Biomed. Mater. Res.*, 1990, **24**, 331–343.
12. Yoshii, S., Kakutani, Y., Nakamura, T., Kitsugi, T., Oka, M., Kokubo, T. *et al.*, Strength of bonding between A-W glass ceramic and the surface of bone cortex. *J. Biomed. Mater. Res.*, 1988, **22**(A), 327–332.
13. Oonishi, H., Hench, L. L., Wilson, J., Sugihara, F., Tsuji, E., Matsuura, M. *et al.*, Quantitative comparison of bone growth behavior in granules of Bioglass®, A-W glass-ceramic, and hydroxyapatite. *J. Biomed. Mater. Res.*, 2000, **51**, 37–46.
14. Kokubo, T., Surface chemistry of bioactive glass-ceramics. *J. Non-Cryst. Solids*, 1990, **120**, 138–151.
15. Sasaki, K., Ishida, H., Okada, Y. and Mitsuda, T., Highly reactive β-dicalcium silicate: V. Influence of specific surface area on hydration. *J. Am. Ceram. Soc.*, 1993, **76**, 870–874.
16. Rodríguez, Rodríguez, J. L., De Aza, M. A. and Pena, S., Reaction sintering of zircon–dolomite mixtures. *J. Eur. Ceram. Soc.*, 2001, **21**, 343–348.
17. Vogan, J. W., Hsu, L. and Stetson, A. R., Thermal barrier coatings for thermal insulation and corrosion resistance in industrial gas turbine. *Thin Solid Films*, 1981, **84**, 75–87.
18. Jansen, F., Wei, X. H., Dorfman, M. R., Peters, J. A. and Nagy, D. R., Performance of dicalcium silicate coatings in hot-corrosive environment. *Surf. Coat. Technol.*, 2002, **149**, 57–61.
19. Liu, X., Tao, S. and Ding, C., Bioactivity of plasma sprayed dicalcium silicate coatings. *Biomaterials*, 2002, **23**, 963–968.
20. Gou, Z. and Chang, J., Synthesis and in vitro bioactivity of dicalcium silicate powders. *J. Eur. Ceram. Soc.*, 2004, **24**, 93–99.
21. Lea, F. M., *The Chemistry of Cement and Concrete* (*3d ed.*). Chemical Publishing Co, New York, 1971.
22. Fisher, H. and Marx, R., Fracture toughness of dental ceramics: comparison of bending and indentation method. *Dent. Mater.*, 2002, **18**, 12–19.
23. Kokubo, T., Kushitani, H., Saka, S., Kitsgi, T., Kitsugi, T. and Yamamuro, T., Solutions able to reproduce in vivo surface structure changes in bioactive glass-ceramics A-W. *J. Biomed. Mater. Res.*, 1990, **24**, 721–734.
24. Greenspan, D. C., Zhong, J. P. and LaTorre, G. P., Effect of surface area to volume ratio in vitro surface reactions of bioactive glass particulates. In *Bioceramics, Vol 7*, ed. Ö. H. Andersson and A. Yli-Urpo. Turku, Finland, 1994, pp. 55–60.
25. Ringe, J., Kaps, C., Schmitt, B., Büscher, K., Bartel, J., Smolian, H. *et al.*, Porcine mesenchymal stem cells: induction of distinct mesenchymal cell lineages. *Cell Tissue Res.*, 2002, **307**, 321–327.
26. Josset, Y., Nasrallah, F., Jallot, E., Lorenzato, M., Dufour-Mallet, O. and Balossier, G., Influence of physico-chemical reactions of bioactive glass on the behavior and activity of human osteoblasts in vitro. *J. Biomed. Mater. Res.*, 2003, **67A**, 1205–1218.
27. Koutsopoulos, S., Synthesis and characterization of hydroxyapatite crystals: a review study on the analytical methods. *J. Biomed. Mater. Res.*, 2002, **62**, 600–612.
28. Chan, C. J., Kriven, W. M. and Yong, F. J., Physical stabilization of the β → γ transformation in dicalcium silicate. *J. Am. Ceram. Soc.*, 1992, **75**, 1621–1625.
29. Groves, G. W., Phase transformations in dicalcium silicate. *J. Mater. Sci.*, 1983, **18**, 1615–1624.
30. Kim, Y. J., Nettleship, I. and Kriven, W. M., Phase transformations in dicalcium silicate: II, TEM studies of crystallography, microstructure, and mechanisms. *J. Am. Ceram. Soc.*, 1992, **9**, 2407–2419.
31. Hulbert, S. F., Bokros, J. C., Hench, L. L., Wilson, J. and Heimke, G., Ceramics in clinical applications: past, present, and future. In *High Technological Ceramics*, ed. P. Vincenzini. Elsevier Science, Amsterdam, 1987, pp. 189–213.
32. Hench, L. L., Bioceramics. *J. Am. Ceram. Soc.*, 1998, **7**, 1705–1728.
33. Currey, J. D. and Brear, K., Hardness, Young's modulus and yield stress in mammalian mineralized tissue. *J. Mater. Sci.: Mater. Med.*, 1990, **1**, 14–20.
34. Morgan, E. F., Yetkinler, N. D., Constantz, B. R. and Dauskardt, R. H., Mechanical properties of carbonated apatite bone mineral substitute: strength, fracture and fatigue behavior. *J. Mater. Sci.: Mater. Med.*, 1997, **8**, 559–570.
35. Hull, D. and Clyne, T. W., *An Introduction to Composite Materials* (*2nd ed.*). Cambridge University Press, Cambridge, 1996.
36. Moya, J. S., Pena, P. and Aza, S. D., Transformation toughening in composites containing dicalcium silicate. *J. Am. Ceram. Soc.*, 1985, **68**, C259–C262.
37. Shi, J. L., Thermodynamics and densification kinetics in solid-state sintering of ceramics. *J. Mater. Res.*, 1999, **14**, 1398–1408.
38. Rice, R. W., Grain size and porosity dependence of ceramic fracture energy and toughness at 22 °C. *J. Mater. Sci.*, 1996, **31**, 1969–1983.
39. Shen, Z., Adolfsson, E., Nygren, M., Gao, L., Kawaoka, H. and Niihara, K., Dense hydroxyapatite–zirconia ceramic composites with high strength for biological applications. *Adv. Mater.*, 2001, **13**, 214–216.

40. Dorozhkin, S. V. and Epple, M., Biological and medical significance of calcium phosphates. *Angew. Chem. Int. Ed.*, 2002, **41**, 3130–3146.
41. Hench, L. L., Splinter, R. J., Allen, W. C. and Greenlee, T. K., Bonding mechanisms at the interface ceramic prothetic materials. *J. Biomed. Mater. Res. Symp.*, 1971, **36**, 117–141.
42. Goshima, J., Goldberg, V. M. and Caplan, A. I., Osteogenic potential of culture-expanded rat marrow cells as assayed in vivo with porous calcium phosphate ceramic. *Biomaterials*, 1991, **12**, 253–258.
43. Yoshikawa, T., Noshi, T., Mitsuno, H., Hattori, M., Ichijma, K. and Takakura, Y., Bone and soft regeneration by bone marrow mesenchymal cells. *Mater. Sci. Eng. C*, 2001, **17**, 19–26.